Syracuse University
SURFACE at Syracuse University

Theses - ALL

5-14-2023

Extended controlled-release of drugs and nanoparticles from shape memory polymers

David Anthony Fikhman
Syracuse University

Follow this and additional works at: https://surface.syr.edu/thesis

Recommended Citation
Fikhman, David Anthony, "Extended controlled-release of drugs and nanoparticles from shape memory polymers" (2023). *Theses - ALL*. 709.
https://surface.syr.edu/thesis/709

This Thesis is brought to you for free and open access by SURFACE at Syracuse University. It has been accepted for inclusion in Theses - ALL by an authorized administrator of SURFACE at Syracuse University. For more information, please contact surface@syr.edu.

Abstract

The ability to externally control release from implants offers a safer and more efficient way of delivering drugs to the body as compared to traditional drug depots that rely upon diffusion and do not allow for a change in dosage after implantation. Previous studies employed magnetic nanoparticle (NP)-loaded shape memory polymer (SMP) films to determine if magnetic actuation could be used to release a model drug (rhodamine B) from strained and unstrained samples and to establish structure/property relationships regarding drug release from SMPs. This previous study was limited by short release time characterization periods (7 hours) and does not provide long-term release information from these scaffolds. To address this limitation, the current study analyzed how magnetic actuation affects release of rhodamine B from both strained and unstrained SMP films with varied chemistries (crosslinked and uncrosslinked) in accelerated hydrolytic (0.1M NaOH), accelerated oxidative (20% H2O2), and 'real time' (PBS) media over 26 days. As a proof-of-concept for further control over release, rhodamine B was first loaded into microparticles (μP), which were subsequently incorporated into SMP scaffolds to evaluate release over time. General trends show that magnetic actuation in samples containing NPs increased release relative to those without. Linear (uncrosslinked) samples release significantly more rhodamine B than crosslinked samples. In these long-term studies, straining samples did not have an effect on release rates compared with non-strained samples. 'Real time' media allowed for the highest measured release. Accelerated oxidative media resulted in the lowest measured release, which is attributed to H_2O_2 oxidation of the rhodamine B. Lastly, incorporation of rhodamine B into microparticles prior to loading into films completely eliminated release of rhodamine B at the given mass used. This work acts as a proof-of-concept for controlling sustained drug delivery by varying SMP chemistry, straining, magnetic NP incorporation, and drug-loaded microparticles.

Extended controlled-release of drugs and nanoparticles from shape memory polymers

by
David Fikhman

B.S. Syracuse University, 2022

Thesis
Submitted in partial fulfillment of the requirements for the degree of Master of Science in Chemical Engineering

Syracuse University
May 2023

Copyright © David Fikhman 2023

All Rights Reserved

Acknowledgements

To start off my acknowledgements, I would like to thank Dr. Mary Beth Monroe for initially letting me into her lab in Spring 2019 to start in Fall 2019. During the last four years I have had a lot of ups and downs in college, and Dr. Mary Beth Monroe fostered a very welcoming environment given circumstances. I've learned a lot under various people, been inspired, and learned various things about many projects. Dr. Mary Beth Monroe has also allowed me to grow both personally and professionally when it comes to research and has supported me throughout my entirety of being in the lab.

My next thank you goes out to everyone who I have worked with in the lab. All the way back to Nakira Christmas being my first mentor for my sophomore year, to Changling Du being my mentor up until I graduated with my bachelor's degree and is still mentoring me to this day even if we aren't working directly together. I want to also thank Maryam Ramezani, Anand Vakil, Henry Beaman, Jingyi Liu, Ellen Shepherd, Natalie Petryk, and Nghia Thai as other members of the lab who have taught me a variety of skills and helped me along the way by teaching me. Lastly from the MBM Lab Group, I would like to thank Leo Saldanha for being my mentee this last year, helping me in many ways and committing himself to growth in research and towards the project. Leo has also taught me a lot when it comes to mentoring.

I would like to thank Dr. Monroe, Dr. Rachel Steinhardt, Dr. Era Jain, and Dr. Julie Hasenwinkel for being a part of the committee. I have had a few of you as professors, I've had talks with many of you outside of classes, and some have participated in other defenses for my past lab mates and I thank you for the support I am receiving and that they have received.

For Dr. Era Jain, I thank you and Paul Sagoe for making me microparticles encapsulating rhodamine B for initial research into how microparticles affect release through polymer films. I appreciate that you both wrote and edited the materials and methods section regarding the synthesis of the microparticles, and for doing this on top of everything else you both have going on.

Lastly, I would like to thank my mother for supporting me to no bounds throughout university. Thank you everyone again for supporting me and offering me experiences I never knew I would have.

Table of Contents

List of Illustrative Material

1. Introduction

Drug delivery systems include oral, intravenous, and dermal routes. Oral delivery is the most common route of administration, followed by intravenous.[1] The benefit of oral delivery lies in convenience, cost, and safety, while intravenous allows for more precise dosing.[2][3] However, oral delivery can result in variable absorption, depending on an individual's stomach acid or how much food they have eaten. Additionally, intravenous administration can only be administered by a medical professional, results in uneven drug distribution within the body, and can cause patient sensitivity and discomfort with repeated insertions into the veins.[4] Dermal routes, such as drug depots, can offer a way to provide controlled and sustained drug release and can eliminate the need for frequent dosing. However, once implanted, drug depots do not allow for changes in dosage unless they are taken out.[5]

In general, drug depots can increase efficacy of systemic drug delivery by bypassing the limitations of oral and intravenous delivery (e.g., during delivery of hormonal birth control).[6] Drug depots also offer options for targeted drug delivery. Targeted drug delivery is a method to deliver drugs to a specific site in the body through the use of implants, nanoparticles, hydrogels, or other systems engineered to carry a drug and release it in a controlled manner at a desired site. This method can reduce systemic effects of drugs and is therefore employed for applications such as cancer treatments, where chemotherapeutics (e.g., doxorubicin) are locally released next to a tumor site.[7] Both systemic and localized delivery rates can be modified in drug depots using sustained drug delivery, which offers routes to administer a drug slowly and over a longer period of time compared to oral and intravenous delivery. Sustained drug

delivery can help control drug concentration in the bloodstream and reduce the frequency of dosing.[8]

Previous work by Vakil et al. employed a shape memory polymer (SMP)-based implant to provide controlled drug delivery.[9] SMPs are defined as a class of smart materials that can remember a primary shape, be programmed into a temporary shape, and return to the primary shape once exposed to external stimulus, such as heat, light, or a magnetic field.[10] These SMPs were designed to release drugs upon application of a magnetic field by incorporating magnetic nanoparticles (NPs) and a model drug (rhodamine B, molar mass of 479.02 $g \cdot mol^{-1}$).[9] While rhodamine B is not a perfect model of traditional drugs, which are often very hydrophobic, it offers a means of easy detection for release by its absorbance peak at 555 nm, enabling rapid characterization of release based on multiple scaffold variables. Vakil, et al. compared release from static unstrained samples and strained samples that changed shape under the magnetic field.[9] Straining is defined as programming the polymer into a new shape by heating it above its glass transition temperature, stretching it lengthwise, and holding the stretched position during cooling to fix the secondary shape. The incorporated NPs were excited due to the alternation the magnetic field, with caused localized heating of strained samples past their wet glass transition temperature in solution, causing them to return to their original shape and release the trapped drug. Thus, the external magnetic field offers a way to remotely control drug release to create more precise and safer drug delivery pathways.[11]

In this study, we learned that non-crosslinked linear SMP films had faster release rates than crosslinked thermoset films. When looking at strained vs. unstrained

samples, strained samples released less drug that corollary unstrained samples. Magnetic nanoparticle excitation by magnetic field aided in drug diffusion out of the polymer network by increasing the polymer temperature. Higher loading of magnetic NPs resulted in higher drug release during exposure to the same magnetic field than lower concentrations in the same field.[9]

This previous study provided promising results but was limited by short characterization time frames (7 hours) and simple, direct incorporation of drugs into the polymer scaffolds, which reduces control over release profiles. Thus, the current work follows Vakil et al. in their use of SMPs to understand how alternating magnetic fields affect drug release from linear and crosslinked SMPs by characterizing long-term release over 26 days in varying degradation media. Additionally, NP release was characterized, and rhodamine B release from drug-encapsulated microparticles was assessed as a means of further controlling release. Using rhodamine B as a model drug, we can determine how these variables affect drug and magnetic nanoparticle release over long time frames to enable rational design of targeted drug delivery systems in the future. We initially hypothesized that: (1) Polymers with linear chains should release more rhodamine B than crosslinked polymer networks due to easier diffusion out of linear networks; (2) Polymers with NPs should release more than corollary samples without NPs due to effects of magnetic field on exciting the particles, locally heating samples, and increasing diffusion; (3) Strained samples should release less than unstrained samples due to reduced space between strained polymer chains to reduce diffusion; (4) accelerated hydrolytic and oxidative media should result in faster release to enable longer-term outlooks on release over time; and (5) incorporating drug

into microparticles prior to addition to polymers should offer another layer against release of rhodamine B and slow down its release.

2. Materials and Methods

2.1 Materials

Sodium borohydride, ferric chloride hexahydrate, phosphate-buffered saline tablets (PBS), rhodamine B, 30% hydrogen peroxide (H_2O_2), methanol, hexamethylene diisocyanate (HDI), triethylene glycol (TEG), polypropylene glycol (2000 Da, PPG), N', N', N, N-tetrakis-2-hydroxypropyl ethylenediamine (HPED), and dibutyl(tin)dilaurate (DBTDL) were purchased from Fisher Scientific (Waltham, MA, USA) as reagent grade. TEG, PPG, HPED, and HDI were dried overnight at 40°C in -30 inHg before being used inside a moisture-controlled glove box.

For microparticles, poly(ethylene glycol)-methyl ether-block -poly(lactide-co-glycolide) (PEG-PLGA 50:50, M_n PEG 2000 and PLGA 10,000 Da), was purchased from Sigma Aldrich (St. Louis, MO, USA). Rhodamine B, polyvinyl alcohol (PVA) (87-89% hydrolyzed, high molecular weight), polyvinyl chloride (PVC) tubing, syringes (glass and plastic), syringe needles, polytetrafluoroethylene (PTFE)-based consumables (e.g., evaporating dish), and magnetic stirring bars were obtained from Fisher Scientific. All other chemicals and reagents used in this study were of analytical grade.

2.2 Nanoparticle Synthesis

Magnetic nanoparticles were synthesized as previously described.[8] In a 250 mL beaker, a ferric chloride ($FeCl_3.6H_2O$) solution at 0.1 M was added dropwise into a solution of sodium borohydride ($NaBH_4$) at 2.5 M in deionized water in a ratio of 4:1. While the ferric chloride solution was being added, the solution was stirred at 1050 rpm on a magnetic stir plate (Fisher Scientific, Waltham, MA, USA). The reaction was

carried out until bubbling stopped. The magnetic particles were allowed to settle, and then the solution was transferred into a centrifuge tube to be centrifuged at 10000 ×g for 10 minutes. After centrifuging, the supernatant was poured off and replaced with fresh deionized (DI) water. This step was repeated four times, twice with DI water and twice with methanol. The washed particles were then dried at 50°C overnight, and clusters were broken up the following day. The size of the particles was determined by dynamic light scattering (DLS) using a Zetasizer Ultra (Malvern Panalytical, Westborough, MA, USA). To do this, 1 mg of particles were added to 5 mL of DI water in a 10x10 polystyrene cell and sonicated for 5 minutes. Particle sizes were confirmed using the DLS.

2.2 Microparticle Synthesis

Polymeric microparticles (µPs) were fabricated using a modified phase separation method based on coaxial flow technology. In short, a 5% w/v organic phase was prepared by fully dissolving 25 mg of PEG-PLGA in 500 µl of dichloromethane (DCM). Similarly, a 5% w/v aqueous phase was created by dissolving 5 mg of polyvinyl alcohol (PVA) in 100 ml of deionized water. To synthesize rhodamine B-loaded microparticles (µPs), 5 ul of 5 mg/ml rhodamine B dye in deionized water was added to the organic phase. The resulting organic phase, which now contained 1% v/v rhodamine B, was placed in a glass syringe, while the aqueous phase (5% w/v PVA, 20 ml) was placed in a plastic syringe. The two syringes were then coaxially connected using a coaxial needle construct and a luer lock PVC tubing, and the phases (organic and aqueous) were concurrently injected via a laterally generated orifice into a PTFE

evaporation dish containing a PVA bath (5% w/v, 5 ml) at respective flow rates of 0.5 ml/hr and 20 ml/hr.

The collected emulsion was constantly stirred with a magnetic stirrer at a rate of 600 RPM until both volumes were completely injected. Moreover, the synthesized microparticles were allowed to stir for another hour for complete evaporation of the DCM. Following this, the microparticle suspension was collected and washed three times with deionized water at (100 ×g, 5 mins) to remove the residual PVA using a 50 mL centrifuge tube. The pelleted µPs were finally redispersed in a 2 ml tube using 0.5 ml deionized water and freeze-dried for further studies.

2.4 Polymer Synthesis

Nine different formulations, 4 of two different chemistries plus one additional µP-loaded sample, of polymer films were made in order to test effects of linear vs. crosslinked polymers, strained vs. unstrained samples, rhodamine, magnetic NPs, and rhodamine B-loaded µPs on release in various media and under an alternating magnetic field, **Table 1**. The two chemistries were HDI-TEG-PPG (linear polymer) and HDI-TEG-HPED (crosslinked polymer) and were dubbed PPG and HPED films, respectively. Control samples of PPG films were made by mixing 2.353 g HDI, 1.585 g TEG, and 4.062 g PPG, in that order, followed by 2 drops of DBTDL as catalyst from a pipette. HPED control films were made by mixing 4.462 g HDI, 1.793 g TEG, and 1.743 g HPED, in that order. The polymers were prepared in a moisture-controlled glovebox (Labconco, Kansas City, MO, USA), ensuring that moisture levels were kept under 250 ppm for PPG films and under 300 ppm for HPED films to prevent isocyanate reactions

with water in the atmosphere. After being mixed in the glovebox, samples were extracted and placed into a speed mixer (Flacktek, Landrum, SC, USA) at 3500 rpm for 30 seconds. After being speed mixed, samples were polymerized in a 50°C oven for 48 hours. For samples containing only rhodamine B, 5 mg of rhodamine was added to the speed mix cup before being placed into the glovebox, and then the above steps were carried out as described. For samples with only magnetic nanoparticles, 50 mg of nanoparticles were added to the speed mix cup and then the protocol was carried out as described. Films containing both nanoparticles and rhodamine had both 50 mg of nanoparticles added and 5 mg of rhodamine added before sample preparation. Films containing microparticles with a loading of 5 mg of rhodamine B in them had 3 mg of microparticles added before preparation.

Table 1: Chemical compositions by mass and catalyst amount. R: Rhodamine; NP: nanoparticles; µP: microparticles; HDI: hexamethylene diisocyanate; TEG: triethylene glycol; PPG: poly(propylene glycol); HPED: hydroxypropyl ethylene diamine; DBTDL: dibutryltin diluarate

Sample Name	HDI (g)	TEG (g)	PPG (g)	HPED (g)	DBTDL (drops)	Rhodamine (mg)	NPs (mg)
PPG	2.353	1.585	4.062	0	2	0	0
NP PPG	2.353	1.585	4.062	0	2	0	50
R PPG	2.353	1.585	4.062	0	2	5	0
RNP PPG	2.353	1.585	4.062	0	2	5	50
HPED	4.462	1.793	0	1.743	0	0	0
NP HPED	4.462	1.793	0	1.743	0	0	50
R HPED	4.462	1.793	0	1.743	0	5	0
RNP HPED	4.462	1.793	0	1.743	0	5	50
µP PPG	2.353	1.585	4.062	0	2	3 mg µP	0

2.5 Thermomechanical Testing

2.5.1 Tensile Testing

Dog bone samples (n = 3, 6.25 mm in length and 1.5 mm in width, with thickness measured for each using calipers) were loaded onto the tensile tester and strained at a rate of 10 mm/min until failure. The resulting stress-strain curves were used to measure ultimate tensile strength (maximum stress), elastic modulus (slope in linear region of curve), and ultimate elongation (maximum strain).

2.5.2 Thermogravimetric Analysis (TGA)

Thermal degradation behavior was determined using TGA. Samples were heated at 10°C/min and the temperature at which 3% degradation occurs was determined using the TA Instruments Universal Analysis 2000 software.

2.5.3 Differential Scanning Calorimetry (DSC)

To find the glass transition temperature (Tg) and melting point (Tm) of each polymer, samples (~5 mg, n = 3) were placed in DSC T_{zero} aluminum pans and subjected to the following thermal cycle in a DSC: samples were cooled to -40°C at 10°C/min, kept isothermally for 2 minutes, cooled to 50°C at a rate of 2°C/min, and then heated to 120°C at 10°C/min. Tg was calculated as the mid-point of the endothermic inflection point, and Tm (if applicable) was calculated as the minimum of the endothermic dip in the second heating run of the resulting thermograms.

2.5.4 Dynamic Mechanical Analysis (DMA)

Dog bone samples (n = 1) were cut from each polymer film. Selected formulations were subjected to the following cycle in DMA. Samples were equilibrated at 60°C and held isothermally for 10 minutes. The cycle was set to abort if the PPG samples were strained more than 40%, or if the HPED samples were strained more than 20%. If an abort occurred, the first "cycle" ended, but the remaining steps were still carried out. Next, the force was ramped up at 0.03 N/min up to 18 N, and then the temperature was ramped down at -2°C/min to -5°C. Samples were held isothermally for 10 minutes. The force was then ramped down at -0.1N/min to 0.01N, and the temperature was ramped up at 2°C/min to 60°C and held isothermally for 10 minutes. Another abort was at the same strain % previously mentioned, ending the second "cycle", but still continuing with the next cycle. The second cycle was repeated two more times. Shape fixity and shape recovery were calculated from the resulting data in the third cycle using the following equations:

Shape Fixity: $R_r(N) = \frac{\epsilon_m - \epsilon_p(N)}{\epsilon_m - \epsilon_p(N-1)} \; X \; 100\%$ Equation 1

Shape Recovery: $R_r(N) \; = \frac{\epsilon_u}{\epsilon_m} X \; 100\%$ Equation 2

Where ϵ_m = maximum strain at loading, ϵ_p = remaining strain after recovery (permanent strain), and ϵ_u = strain after unloading (fixed shape).

2.6 Rhodamine B Release

To begin the experiment, cylindrical oval shapes (n = 6/media type, 18 total; 18.42 mm x 10.04 mm) were cut from each polymer film using a hydraulic press. Media,

including 0.1M NaOH (accelerated hydrolytic), 20% H_2O_2 (accelerated oxidative), and PBS ('real-time'), was prepared, and 6 mL was poured into vials for each sample. For each formulation, a subset of samples was strained lengthwise by 40% (PPG) and 20% (HPED) prior to testing (n = 3 per condition). Samples were incubated at 37°C over 24 hours, and then the media and sample were poured out into a 6 mL holder that was placed under an alternating magnetic field for 10 minutes using a previously described setup.[9] The sample was placed back into the vial with 6 mL of fresh media and incubated at 37°C for another 24 hours. Media with released rhodamine (500 µL) after magnetic field exposure was pipetted into a glass cuvette for ultraviolet-visible light (UV-vis, Evolution 60, Thermo Scientific, Waltham, MA, USA) spectroscopy analysis to determine the concentration and mass of rhodamine B released based on calibration curves obtained in the three media types. Measurements were taken daily for the first 5 days of the experiment and then every 3 days afterwards until Day 26.

2.7 Magnetic Particle Release

After samples were placed under a magnetic field for 10 minutes, the media was pipetted into centrifuge tubes for storage. The media was then analyzed via DLS to determine whether nanoparticles were released into the media at each time point.

2.8 Statistical Analysis

Data is presented as average ± standard deviation. ANOVA with Turkey's post hoc was used to compare study measurements and determine statistical significance, set as $p<0.05$.

3. Results and Discussion

3.1 Thermomechanical Properties

Every sample except for µP PPG had been previously characterized in terms of thermomechanical properties.[8] Properties were reassessed here to ensure that new samples had comparable properties as those previously reported and to characterize the new µP PPG sample, **Table 2**. Overall, properties were comparable to previously reported values.

General trends include: UTS is decreased with the addition of rhodamine B and/or NPs in PPG samples, and it is decreased with rhodamine addition in HPED samples. Elastic modulus (E) decreases in PPG samples with rhodamine B and/or NP addition, while it decreases in HPED samples with rhodamine B addition. Ultimate elongation (UE) decreases in both chemistries with the addition of NPs. These trends in mechanical properties can be attributed to how the NPs, rhodamine B, and microparticles are incorporated into the polymer network, as they may alter intermolecular bonding between chains and/or chain organization to reduce tensile properties.

The 3% degradation temperature and Tg remains constant with rhodamine B, NP, and microparticle addition in both chemistries. In semi-crystalline PPG samples, Tm is similar after additions. HPED samples are amorphous and do not have a Tm. Shape fixity of PPG samples remained constant after the addition of rhodamine B and/or NPs. They also exhibit similar shape recovery, except that PPG with NPs has an increase in shape recovery. HPED samples show high recovery and fixity in controls and samples with NPs; however, addition of rhodamine B (without and with NPs) caused the samples

to break before reaching full elongation, preventing full characterization via DMA. This may result be attributed to the crosslinked network of HPED being stiffer than the linear PPG, which does not allow it to elongate as much, as is reflected in the lower ultimate elongation of these samples. The incorporation of rhodamine B and/or NPs reduces sample stiffness and strength, which limits shape memory properties. Similarly, since there was only a sample size of 1 for fixity and recovery, it would be appropriate to do further samples to examine if trends are occurring from rhodamine B and nanoparticles for both chemistries.

Table 2. Thermomechanical properties of synthesized SMP films. UTS: Ultimate tensile strength; E: elastic modulus; UE: ultimate elongation; 3% Deg: temperature at which 3% thermal degradation occurs; Tg: glass transition temperature; Tm: melting temperature; R_f: Shape fixity; R_r: Shape recovery; n=3 for mechanical and thermal properties, mean ± standard deviation displayed; n = 1 for shape memory properties (R_f and R_f).

Sample Name	UTS (MPa)	E (MPa)	UE (%)	3% Deg (°C)	Tg (°C)	Tm (°C)	R_f and R_r (%)
PPG	14.3 ± 1.2	0.70 ± 0.10	1203 ± 81	278 ± 3	90 ± 1	93 ± 1	-
NP PPG	15.0 ± 2.8	0.70 ± 0.12	679 ± 524	272 ± 2	87 ± 3	91 ± 2	89 & 73
R PPG	14.7 ± 2.7	0.63 ± 0.08	1275 ± 189	277 ± 1	90 ± 1	94 ± 1	95 & 63
RNP PPG	8.4 ± 0.2	0.62 ± 0.10	745 ± 294	277 ± 1	91 ± 2	95 ± 1	94 & 60
HPED	30.0 ± 2.0	8.1 ± 3.7	1092 ± 401	266 ± 1	36 ± 1	-	-
NP HPED	40.0 ± 2.5	6.9 ± 2.0	293 ± 21	267 ± 1	37 ± 1	-	99 & 82
R HPED	15.9 ± 5.9	4.5 ± 1.9	174 ± 25	266 ± 1	33 ± 1	-	-
RNP HPED	20.8 ± 14.6	5.4 ± 0.9	374 ± 73	269 ± 1	32 ± 1	-	-
µP PPG	13.0 ± 1.7	0.56 ± 0.08	250 ± 120	272 ± 2	91 ± 1	93 ± 1	89 & 66

3.2 Magnetic Nanoparticle Release

After being analyzed via DLS, the presence of magnetic NPs in surrounding solution at each release time point was analyzed, **Table 3**. Every sample that contained NPs consistently released NPs at all time points and in all three media formulations

throughout the 26-day experiment. Future work should focus on characterizing specific NP concentrations over time and cytocompatibility of released NPs.

Table 3: Magnetic nanoparticle presence in PBS, 0.1M NaOH, and 20% $H2O_2$, n = 3 per media. ☑: released NPs detected via DLS; ✕: no NPs detected via DLS.

Sample Name	Media	Day 1	Day 2	Day 3	Day 4	Day 5	Day 8	Day 11	Day 14	Day 17	Day 20	Day 23	Day 26
PPG	PBS	✕	✕	✕	✕	✕	✕	✕	✕	✕	✕	✕	✕
	NaOH	✕	✕	✕	✕	✕	✕	✕	✕	✕	✕	✕	✕
	H_2O_2	✕	✕	✕	✕	✕	✕	✕	✕	✕	✕	✕	✕
NP PPG	PBS	☑	☑	☑	☑	☑	☑	☑	☑	☑	☑	☑	☑
	NaOH	☑	☑	☑	☑	☑	☑	☑	☑	☑	☑	☑	☑
	H_2O_2	☑	☑	☑	☑	☑	☑	☑	☑	☑	☑	☑	☑
R PPG	PBS	✕	✕	✕	✕	✕	✕	✕	✕	✕	✕	✕	✕
	NaOH	✕	✕	✕	✕	✕	✕	✕	✕	✕	✕	✕	✕
	H_2O_2	✕	✕	✕	✕	✕	✕	✕	✕	✕	✕	✕	✕
RNP PPG	PBS	☑	☑	☑	☑	☑	☑	☑	☑	☑	☑	☑	☑
	NaOH	☑	☑	☑	☑	☑	☑	☑	☑	☑	☑	☑	☑
	H_2O_2	☑	☑	☑	☑	☑	☑	☑	☑	☑	☑	☑	☑
HPED	PBS	✕	✕	✕	✕	✕	✕	✕	✕	✕	✕	✕	✕
	NaOH	✕	✕	✕	✕	✕	✕	✕	✕	✕	✕	✕	✕
	H_2O_2	✕	✕	✕	✕	✕	✕	✕	✕	✕	✕	✕	✕
NP HPED	PBS	☑	☑	☑	☑	☑	☑	☑	☑	☑	☑	☑	☑
	NaOH	☑	☑	☑	☑	☑	☑	☑	☑	☑	☑	☑	☑
	H_2O_2	☑	☑	☑	☑	☑	☑	☑	☑	☑	☑	☑	☑
R HPED	PBS	✕	✕	✕	✕	✕	✕	✕	✕	✕	✕	✕	✕
	NaOH	✕	✕	✕	✕	✕	✕	✕	✕	✕	✕	✕	✕
	H_2O_2	✕	✕	✕	✕	✕	✕	✕	✕	✕	✕	✕	✕
RNP HPED	PBS	☑	☑	☑	☑	☑	☑	☑	☑	☑	☑	☑	☑
	NaOH	☑	☑	☑	☑	☑	☑	☑	☑	☑	☑	☑	☑
	H_2O_2	☑	☑	☑	☑	☑	☑	☑	☑	☑	☑	☑	☑
µP PPG	PBS	✕	✕	✕	✕	✕	✕	✕	✕	✕	✕	✕	✕
	NaOH	✕	✕	✕	✕	✕	✕	✕	✕	✕	✕	✕	✕
	H_2O_2	✕	✕	✕	✕	✕	✕	✕	✕	✕	✕	✕	✕

3.3 Rhodamine B Release

After experimentation, all data was plotted over time to determine effects of chemistry (PPG vs. HPED), straining samples prior to characterizing release, magnetic NP incorporation, and rhodamine B loading into microparticles to understand how each

factor affects prolonged release. To accelerate release characterization, subsets of samples were incubated in 0.1M NaOH (accelerated hydrolytic degradation) and 20% H_2O_2 (accelerated oxidative degradation) in addition to the more physiologically relevant PBS. **Figure 1** displays the % release of rhodamine B from each film, assuming that samples were loaded with a total of 287 µg. This value was calculated by setting a ratio of the volume of the sample to the volume of the entire film as compared with the ratio of rhodamine B in the entire film.

Comparing final release from RNP PPG strained and unstrained samples in PBS shows us that unstrained samples release more than strained samples in 'real-time' media, which was expected based on strained chain conformations that inhibit release. However, most formulations had similar release from corollary strained and unstrained samples, both at the final time point (visible in **Figure 1**) and during days 1-11 (determined by diffusion coefficients in **Table 4**). We hypothesize that the strained samples regain their primary, unstrained shapes earlier in the study to minimized effects of straining in these long-term studies. We also see that unstrained samples with NPs release more than non-NP containing samples at the final time point, as expected based on an increase in temperature upon exposure to a magnetic field that increases diffusion out of the samples. However, in strained samples, the effects of NPs on release are somewhat lessened, which correlated with overall lower release from these samples. Additionally, diffusion coefficients at earlier time points were similar between samples with and without NPs. When comparing HPED and PPG samples, release is lower out of crosslinked HPED both initially and over the full 26 days. We attribute this result to the density of the matrix, inhibits rhodamine diffusion to slow release.[9]

Table 4. Diffusion coefficients (mg/day) over days 1-11 for unstrained and strained rhodamine B containing samples in various media.							
		PBS		**0.1M NaOH**		**20% H_2O_2**	
Sample Type		**R**	**RNP**	**R**	**RNP**	**R**	**RNP**
Unstrained	PPG	9.72	9.91	4.31	9.02	2.71	1.3
	HPED	0.96	0.47	0.39	1.22	2.71	3.50
Strained	PPG	11.7	10.24	10.64	11.8	5.60	0.07
	HPED	0.76	0.73	0.60	0.92	0.54	4.01

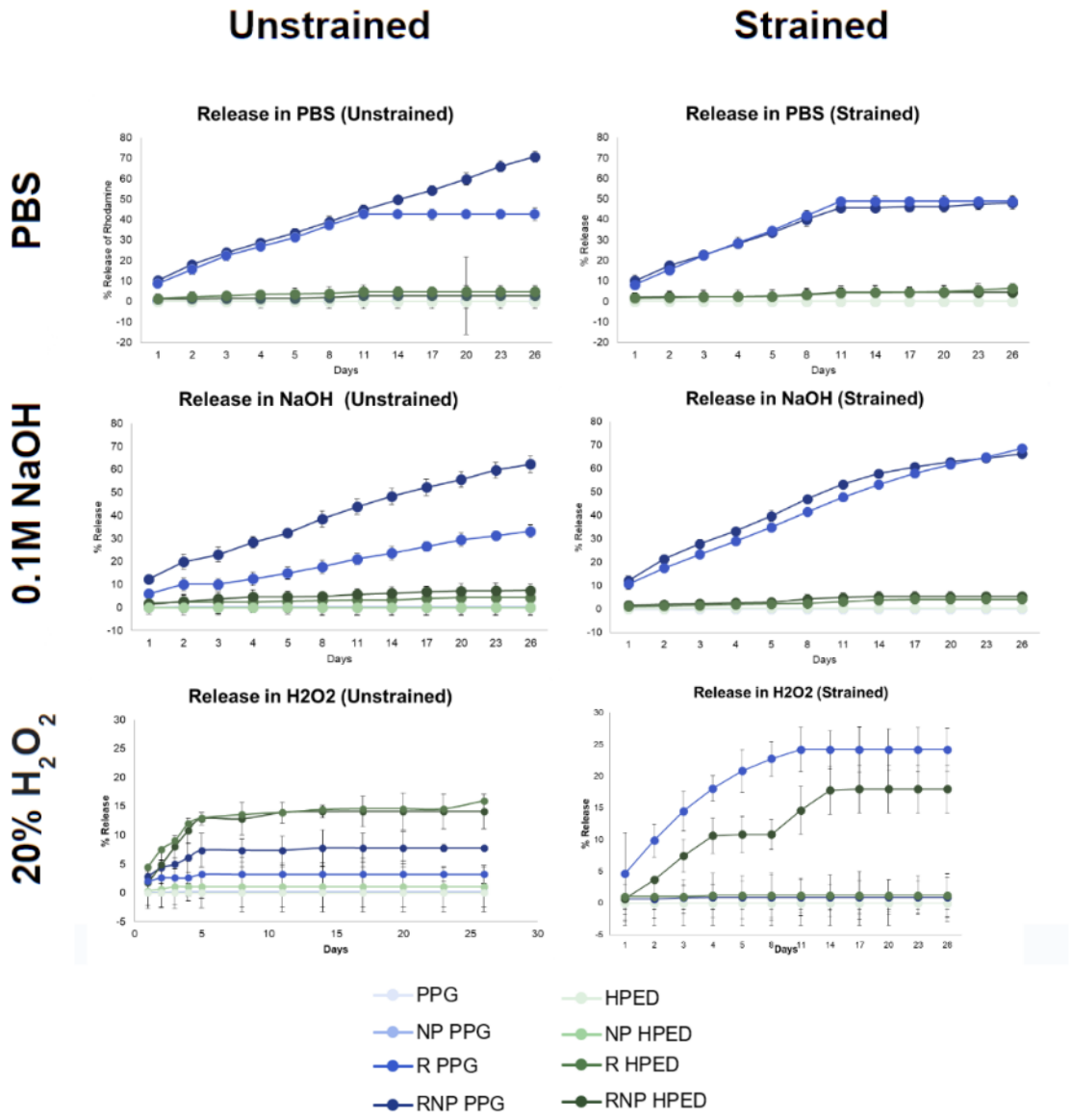

Figure 1. Rhodamine B release in unstrained (left) and strained (right) samples after magnetic field application and incubation in PBS (top row), 0.1M NaOH (middle row), and 20% H_2O_2 bottom row. n = 3, mean ± standard deviation displayed.

When comparing release from unstrained and strained R PPG samples in NaOH, strained samples released more overall than unstrained. This can be observed in both **Figure 1** for overall release and **Table 4** for release from Days 1-11, where the diffusion coefficients are higher for strained formulations. This trend is unexpected and warrants further investigation, specifically into when the effects of straining disappear over the course of the experiment. When samples are strained, they store potential energy within their structure, and when they return to their original shape, that energy is released, which may result in more release or diffusion of molecules incorporated into their structure to explain these trends.[12] Most formulations had similar release from corollary strained and unstrained samples in NaOH. A similar trend of NP-containing samples releasing more was observed in unstrained samples in NaOH, both initially and at the final time point. However, within the strained sample release in NaOH, NP samples initially release more, but at later time points, the non-NP samples release comparable amounts of rhodamine B. In terms of the effects of chemistry on release in NaOH, HPED samples released less rhodamine B than PPG samples, which matches trends observed in PBS.

Within accelerated oxidative media, both unstrained and strained samples exhibit lower release of rhodamine B than in the other media types. This can be shown by **Figure 1** and **Table 4**, where the diffusion coefficients are lower for all samples except for RNP HPED. This result is attributed to rhodamine B being oxidized by H_2O_2, which gives it a clear color and makes it undetectable at 555 nm wavelength on the UV-vis spectra.[13] Additionally, we can still see that there is higher release from non-NP containing PPG samples as compared with release from NP PPG. This result correlates

with qualitative observations of ‘bleaching’ in the RNP PPG samples. This effect may be due to reactions between iron in the magnetic NPs and H_2O_2 to increase reactive oxygen species and speed up rhodamine B oxidation.[14] Similarly, RNP HPED samples released significantly more than any other rhodamine-containing HPED sample, because HPED can be oxidatively degraded.[15] Within this accelerated oxidative environment, the NP-containing HPED samples are completely degraded by Day 17 due to the increase in ROS with the presence of NPs. In all cases, PPG samples release more rhodamine B than HPED samples in H_2O_2, which is generally expected based on diffusion out of linear polymers (PPG) vs. crosslinked polymers (HPED). However, PPG samples are oxidatively stable, whereas HPED samples are degraded oxidatively, which could have competing effects on release in oxidative media.[16]

To enable direct comparisons, each tested variable was plotted against each other in terms of final release at 26 days in **Figure 2**. The initial hypothesis was that accelerated degradation media would result in faster drug release; however, statistically PBS and NaOH are very similar and H_2O_2 significantly decreased release, **Figure 2a**. Both polymer formulations are highly hydrolytically stable, which explains why PBS and NaOH had similar release profiles.[15-16] The oxidation of rhodamine B by H_2O_2 reduced apparent release amounts to skew this data towards lower drug release. Based on prior work, we hypothesized that strained samples would have lower release; however, as shown in **Figure 2b**, straining did not have a significant effect on release in these long-term studies. Thus, after early time points, strained samples likely return to their original shapes during magnetic actuation to eliminate effects of straining in the

long term. Inclusion of magnetic NPs into samples resulted in significantly higher release, which was expected, **Figure 2c**. Lastly, **Figure 2d** shows that there is statistical decrease in release from HPED as compared with PPG samples, which was expected based on reduced diffusion from the crosslinked HPED network.

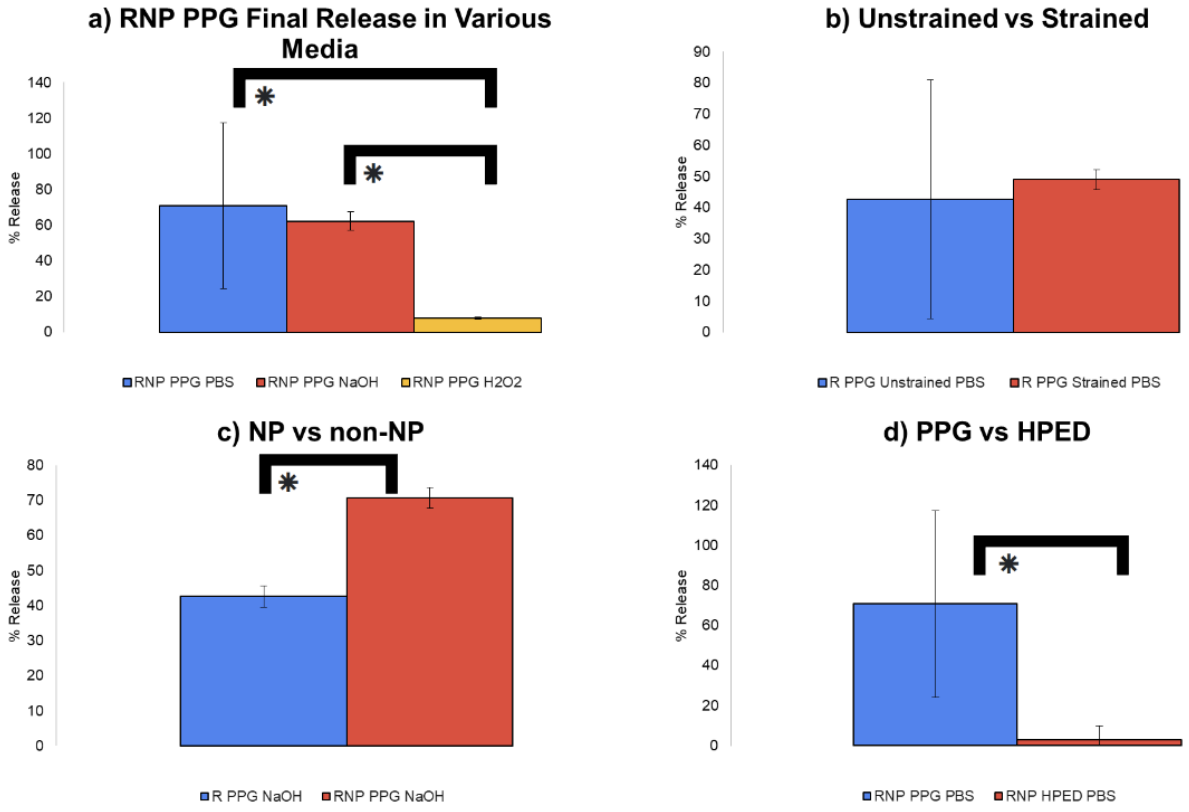

Figure 2. Rhodamine B release at 26 days. a) Comparison between release from RNP PPG in PBS, NaOH, and H_2O_2, b) comparison between release from unstrained and strained R PPG samples in PBS, c) comparison between PPG samples with and without mnps in PBS, d) comparison between release from RNP containing PPG and HPED samples in PBS. N = 3, mean ± standard deviation displayed. *p<0.05 between formulations under brackets.

While these experiments expand our understanding of drug release from SMP samples, some considerations should be made in future work. Before the addition of rhodamine B, it may be apt to form rhodamine-hexahydrate in the presence of water. If

incorporated into samples as a hexahydrate, it may cause foaming to occur due to a reaction between the water and isocyanates to form carbon dioxide bubble during curing. We did not observe bubble formation during sample preparation, but drying the rhodamine B in future studies as a precaution could ensure that this reaction does not occur. Additionally, samples can be washed after their fabrication to evaluate their initial release before long-term characterization. Similarly, they may be washed afterwards to quantify how much rhodamine B or drug is remaining. Finally, rhodamine B was used here due to its low cost and ease of characterization, but it is not a perfect model drug due to its relatively high hydrophilicity. Using the principles gained in these experiments, future work could be conducted to evaluate release of a more relevant drug, such as doxorubicin (a chemotherapeutic) or 6-mercaptopurine (an immunosuppressant).

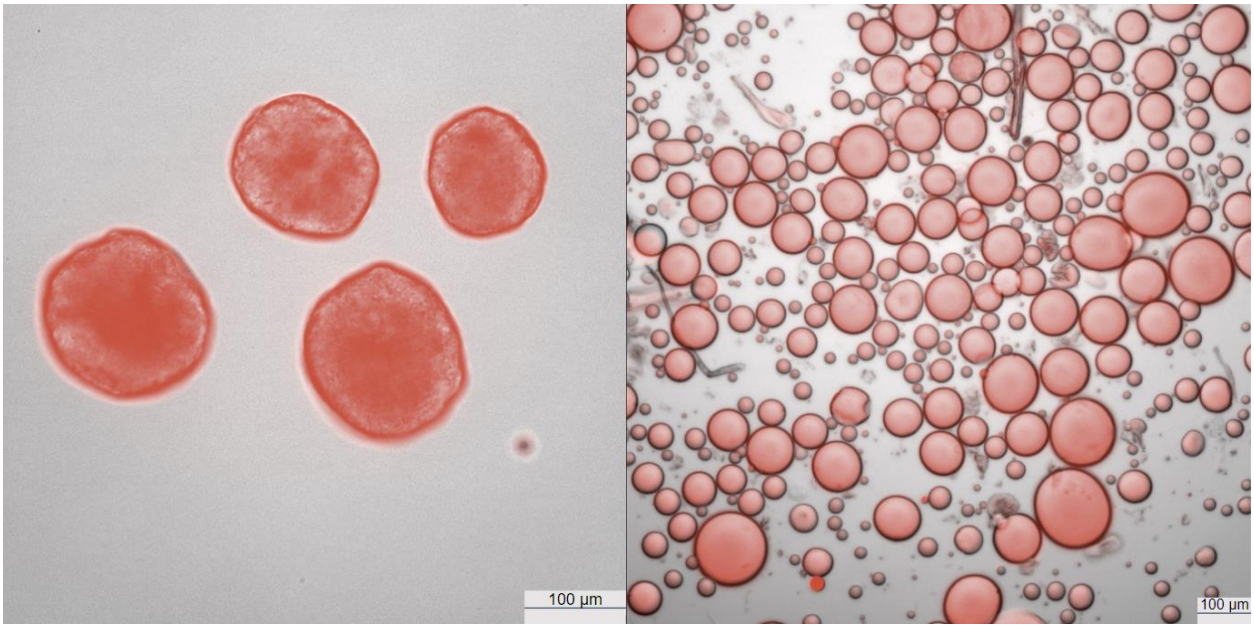

Figure 3. RhoB-µPs (left and right) with an average diameter of 175 µm. Scale bar is 100 nm.

A preliminary experiment was conducted to analyze the ability to control release of rhodamine B from µP's (**Figure 3**) incorporated into PPG samples, **Figure 4**. Over

the course of the 26 days, the µP PPG samples released no rhodamine, while R PPG samples released 69% of the incorporated rhodamine. We anticipated that encapsulation of rhodamine B into uP's before loading it into SMPs would slow diffusion out of the samples by providing an additional barrier for release. However, the complete lack of release was unexpected and could be attributed to many factors. The first factor is relatively low loading of rhodamine B within the uP PPG samples, which may have reduced rhodamine release concentrations to non-detectable values. This effect, combined with slower diffusion capabilities overall could have resulted in extremely slow release in PBS. The microparticles were synthesized with 0.01 mM rhodamine B solution to theoretically have 5 mg of rhodamine B encapsulated within 3 mg of microparticles. The mass after fabrication was ~13 mg microparticles/0.01 mM rhodamine B. As only 3 mg was able to be incorporated into the films, this value equates to 0.002 mM rhodamine B, or 0.000095 mg/mL, as compared with 0.000497 mg/mL in the direct incorporation samples.

Furthermore, the microparticles were not uniformly spread throughout the entirety of the film, which likely affected release results. Qualitatively, we observed that the microparticles localized more towards the center of films (vs. the surface), which could slow diffusion out of the samples. The electrostatic charge on the microparticles may have affected their aggregation in the films during fabrication.[17] Samples were cut from spots that qualitatively contained the most microparticles based on color. The experiment needs to be repeated, possibly with higher microparticle loading, extra measures to ensure even distribution, and with other media types to evaluate accelerated long-term release. We hypothesize that increased release may be observed

in hydrolytic media, as the PLGA in the microparticles can be hydrolyzed by NaOH to enable faster diffusion of rhodamine B.

4. Conclusions

From these studies, we can see that there is sustained release of rhodamine B from PPG and HPED films over the course of 26 days, with the ability to control release based on chemistry, straining, the addition of NPs, and prior incorporation of rhodamine into microparticles. This work provides a proof-of-concept of remotely releasing drugs from implants via magnetic actuation above the implant site. Future work could focus on finding the most effective time for magnetic actuation above the site and on characterizing release from samples that are separated from the applied magnetic field by skin or other tissues to evaluate the potential of this system for use in targeted drug delivery. Microparticles were used to determine if they could further control the release of rhodamine B from PPG films in PBS. Preliminary results showed that rhodamine B did not release from microparticles encapsulated within films. Future experiments should look at increasing microparticle loading amount and distribution. Another future study should analyze how different geometries (e.g., shorter, square, cylindrical, thinner) of implants affect the diffusion of microparticles, drugs, and/or nanoparticles due to them having different temperature profiles and potentially having more surface area. Overall, these experiments provide a rational framework for design of SMP-based drug delivery systems that could be built upon in future work.

5. References

[1] “The World Medicines Situation | World Health Organization.” [Online]. Available: https://apps.who.int/iris/rest/bitstreams/65092/retrieve

[2] Kim J, De Jesus O. Medication Routes of Administration. [Updated 2023 Feb 12]. In: StatPearls [Online]. Treasure Island (FL): StatPearls Publishing; 2023 Jan-. Available: https://www.ncbi.nlm.nih.gov/books/NBK568677/

[3] Haroutounian, S. and Jensen, T.S., “Chapter 8 - Neuropathic Pain Following Surgery,” *Nerves and Nerve Injury*, vol 2, pp 113-117, 2015.

[4] C. D. Delivery, *Controlling drug delivery*, vol. 8, no. 3. 1999.

[5] Danckwerts M., Fassihi A. “Implantable Controlled Release Drug Delivery Systems: A Review,” *Drug Development and Industrial Pharmacy*, vol 17, issue 11, 1991.

[6] Ashagrachew, T. *et al*, “Targeted Drug Delivery – From Magic Bullet to Nanomedicine: Principles, Challenges, and Future Perspectives,” *J Multidiscip Healthc,* vol 21, pp 1711-1724, June 2021.

[7] Saltzman, W. M., & Fung, L. K. (1997). Polymeric implants for cancer chemotherapy. *Advanced drug delivery reviews*, *26*(2-3), 209–230. https://doi.org/10.1016/s0169-409x(97)00036-7

[8] Zamani, F, *et al*, “Chapter 7 - Nanofibrous and nanoparticle materials as drug delivery systems,“ *Micro and Nano Technologies*, 2017, pp 239-270, 2017

[9] A. U. Vakil, M. Ramezani, and M. B. B. Monroe, “Magnetically Actuated Shape Memory Polymers for On-Demand Drug Delivery,” *Materials*, vol. 15, no. 20, p. 7279, Oct. 2022, doi: 10.3390/ma15207279.

[10] Pisani S, Genta I, Modena T, Dorati R, Benazzo M, Conti B. Shape-Memory

Polymers Hallmarks and Their Biomedical Applications in the Form of Nanofibers. Int J Mol Sci. 2022 Jan 24;23(3):1290. doi: 10.3390/ijms23031290. PMID: 35163218; PMCID: PMC8835830.

[11] Perera, Ayomi S. *et al* "Polymer- Magnetic Composite Fibers for Remote-Controlled Drug Release," *ACS Applied Materials & Interfaces* 2018, 15524-15531.

[12] Christopher B. Cooper, Shayla Nikzad, Hongping Yan, Yuto Ochiai, Jian-Cheng Lai, Zhiao Yu, Gan Chen, Jiheong Kang, and Zhenan Bao, *ACS Central Science,* 2021 *7* (10), 1657-1667. DOI: 10.1021/acscentsci.1c00829

[13] Thao, N.T. *et al*, "Advanced oxidation of rhodamine with hydrogen peroxide over Zn-Cr layered double hydroxide catalysts," *Journal of Science: Advanced Materials and Devices*, vol 2, issue 3, pp 317-325, 2017.

[14] Winterbourn C. C. (1995). Toxicity of iron and hydrogen peroxide: the Fenton reaction. *Toxicology letters*, *82-83*, 969–974. https://doi.org/10.1016/0378-4274(95)03532-x.

[15] Weems, A.C. *et al*, "Shape memory polyurethanes with oxidation-induced degradation: *In vivo* and in vitro correlations for endovascular material applications," *Acta Biomaterialia*, vol 59, pp 33-44, 2017.

[16] Maryam Ramezani and Mary Beth Browning Monroe, *ACS Applied Polymer Materials,* 2022 *4* (3), 1956-1965. DOI: 10.1021/acsapm.1c01808

[17] Zeeb, B. *et al*, "Theoretical and practical considerations in electrostatic depositioning of charged polymers," *Journal of Applied Polymer Science*, vol 131, issue 7.

6. Vita

Education

Chemical Engineering, M.S. 2022-2023
Syracuse University

Chemical Engineering, B.S., 2018-2022
Syracuse University

- *ECS Leadership Scholar*
- *Cum Laude*

RESEARCH

Graduate Researcher, *Syracuse University Monroe Biomaterials Lab,* May 2022 - Present
Extended controlled-release of drugs and nanoparticles from shape memory polymers (SMPs) to understand how polymer films with different variables in various conditions release model drugs.

Undergraduate Research Assistant, *Syracuse University Monroe Biomaterials Lab,* August 2019 - May 2022
Synthesis and characterizing oxidation and thermomechanical properties of various phenolic acids incorporated SMP foams, analyzing the clotting capabilities of these foams and characterizing how blood platelets attach to each, as well characterization of shape memory polymer foam hemostats in *in vitro* hemorrhagic wound models.

Undergraduate Research Assistant, *Syracuse University Bond Research Group,* June 2019 - August 2019
Characterizing CO methanation using PtGAl & PtSnGAl catalysts to understand how different compositions affect the chemical pathway to determine which products become more dominant

---

PUBLICATIONS

C. Du, **D.A. Fikhman**, M.B.B. Monroe, "Shape Memory Polymer Foams with Phenolic Acid-Based Antioxidant Properties," *Antioxidants* (2022). DOI: https://doi.org/10.3390/antiox11061105

C. Du, J. Liu, **D.A. Fikhman**, M.B.B. Monroe, "Shape Memory Polymer Foams With Phenolic Acid-Based Antioxidant and Antimicrobial Properties for Traumatic Wound Healing," *Frontiers* (2022). DOI: 10.3389/fbioe.2022.809361

C. Du, **D.A. Fikhman**, D. Persaud, M.B.B. Monroe, "Dual Burst and Sustained Release of p-Coumaric Acid from Shape Memory Polymer Foams for Polymicrobial Infection Prevention in Trauma-related Hemorrhagic Wounds," *Accepted for Publication at ACS Applied Materials and Interfaces* (2023).

AWARDS

AIChE Freshman Recognition Award
American Institute of Chemical Engineers, September 2019

LEADERSHIP AND SERVICE

Alpha Phi Omega: Professional Service Fraternity, 2020 - Present
- Community service around the area of Syracuse University

American Institute of Chemical Engineers President, September 2019 - April 2020
- Coordinating all activities and events for Chemical Engineering students to come together
- Weekly/monthly meetings to get information out for Chemical Engineers regarding topics in work after college, research and how to get into it, and other opportunities
- Management of organization during time as president, as well as being in charge of elections for the next eBoard

MEMBERSHIP

American Institute of Chemical Engineers	2018 - Present
Order of the Engineer	2022 - Present